DNA Repair 24 (2014) 46–56

Contents lists available at ScienceDirect

DNA Repair

journal homepage: www.elsevier.com/locate/dnarepair

Differential binding kinetics of replication protein A during replication and the pre- and post-incision steps of nucleotide excision repair

Audrey M. Gourdin[a,1], Loes van Cuijk[a,1], Maria Tresini[a], Martijn S. Luijsterburg[b,c,2], Alex L. Nigg[d], Guiseppina Giglia-Mari[e], Adriaan B. Houtsmuller[d], Wim Vermeulen[a,*], Jurgen A. Marteijn[a,*]

[a] Department of Genetics, Cancer Genomics Netherlands, Erasmus MC, Wytemaweg 80, 3015 CN Rotterdam, The Netherlands
[b] Swammerdam Institute for Life Sciences, University of Amsterdam, 1098 SM Amsterdam, The Netherlands
[c] Swammerdam Institute for Life Sciences, University of Amsterdam, Sciencepark 904, 1098 XH Amsterdam, The Netherlands
[d] Department of Pathology, Josephine Nefkens Institute, Erasmus MC, Dr. Molewaterplein 50, 3015 GE Rotterdam, The Netherlands
[e] CNRS, IPBS (Institut de Pharmacologie et de Biologie Structurale), 205 route de Narbonne, F-31077 Toulouse, France

ARTICLE INFO

Article history:
Received 16 June 2014
Received in revised form
24 September 2014
Accepted 26 September 2014
Available online 16 October 2014

Keywords:
RPA
DNA replication
DNA repair
Replication stress
Nucleotide excision repair
DNA damage

ABSTRACT

The ability of replication protein A (RPA) to bind single-stranded DNA (ssDNA) underlines its crucial roles during DNA replication and repair. A combination of immunofluorescence and live cell imaging of GFP-tagged RPA70 revealed that RPA, in contrast to other replication factors, does not cluster into replication foci, which is explained by its short residence time at ssDNA. In addition to replication, RPA also plays a crucial role in both the pre- and post-incision steps of nucleotide excision repair (NER). Pre-incision factors like XPC and TFIIH accumulate rapidly at locally induced UV-damage and remain visible up to 4 h. However, RPA did not reach its maximum accumulation level until 3 h after DNA damage infliction and a chromatin-bound pool remained detectable up to 8 h, probably reflecting its role during the post-incision step of NER. During the pre-incision steps of NER, RPA could only be visualized at DNA lesions in incision deficient XP-F cells, however without a substantial increase in residence time at DNA damage. Together our data show that RPA is an intrinsically highly dynamic ssDNA-binding complex during both replication and distinct steps of NER.

1. Introduction

Replication protein A (RPA), the major eukaryotic single-stranded DNA binding protein, is required for several DNA metabolic processes including replication, repair, recombination and checkpoint activation. RPA is a heterotrimer consisting of 70, 32 and 14 kDa subunits and binds ssDNA with a 5′–3′ polarity [1,2]. RPA was initially identified as a crucial replication factor that, together with replication factor C (RFC) and proliferating cell nuclear antigen (PCNA), regulates the loading and processivity of different DNA polymerases onto the chromatin [3].

During replication in eukaryotes the trimeric sliding clamp PCNA, is loaded around the DNA at the 3′-OH end of the nascent DNA strand by the pentameric complex RFC in an RPA- and ATP-dependent manner in order to facilitate the tethering and processing of DNA polymerases δ and ε [4,5]. In eukaryotes, DNA replication is initiated and propagated from hundreds to thousands of replication sites that, together with associated replication factors, cluster into 'replication foci'. The location, number and size of these replication foci vary throughout S-phase. Three distinct replication patterns can be distinguished, that correspond to DNA synthesis in early S phase (small and discrete foci), mid S-phase (perinucleolar and perinuclear large foci) and late S-phase (large foci) [6].

Besides their function in replication RPA, PCNA and RFC are also essential for nucleotide excision repair (NER), a "cut-and-patch" mechanism that by the coordinated action of more than 30 different proteins, removes a wide variety of helix-distorting DNA lesions,

Abbreviations: ssDNA, single stranded DNA; DDR, DNA damage response; NER, nucleotide excision repair; UV, ultraviolet light; CPDs, cyclobutane pyrimidine dimers; 6-4PPs, 6-4 photoproducts; LUD, local UV-induced DNA damage; FRAP, fluorescence recovery after photobleaching; FLIP, fluorescence loss in photobleaching; HU, hydroxyurea; AraC, cytosine-β-arabinofuranoside.

* Corresponding authors. Tel.: +31 107038169.
E-mail addresses: W.Vermeulen@erasmusmc.nl (W. Vermeulen), J.Marteijn@erasmusmc.nl (J.A. Marteijn).

[1] Both authors contributed equally.

[2] Present address: Department of Human Genetics, Leiden University Medical Center, Einthovenweg 20, 2333 ZC Leiden, The Netherlands.

http://dx.doi.org/10.1016/j.dnarep.2014.09.013
1568-7864/

including UV-induced DNA damages like cyclobutane pyrimidine dimers (CPD) and 6-4 photoproducts dimers (6-4-PP) [7]. NER can be sub-divided into two pathways which are activated by distinct recognition mechanisms. (1) Global genome NER (GG-NER) recognizes DNA damage throughout the genome via the concerted action of two damage recognizing complexes; XPC/HR23B/centrin complex and UV-DDB complex [7–9]. (2) Transcription coupled NER (TC-NER) is only active on the transcribed strand of active genes [10] and is initiated by the stalling of elongating RNA polymerase II on DNA lesions [11]. Following damage recognition, GG-NER and TC-NER converge into a common pathway by recruiting the ten-subunit transcription factor TFIIH that verifies the lesion and locally unwinds the DNA double helix around the lesion [12]. RPA then binds to the undamaged DNA strand and, together with XPA, stabilizes open complex formation, thereby stimulating and coordinating the incision by the endonucleases ERCC1-XPF and XPG [13,14,2]. A 24–32-nucleotide DNA fragment is excised and the undamaged strand is used as a template for DNA repair synthesis [15]. Finally the DNA is sealed by LigaseIII-XRCC1 or Ligase I [16]. *In vitro* and *in situ* experiments have revealed that, following dual incision, RPA remains bound to the DNA substrate where it initiates the recruitment of RFC, PCNA and either the DNA polymerase pol ε, or pol κ and δ [17–19].

In contrast to PCNA and RFC, which only play a role in the post-incision steps of NER, RPA is implicated in both the pre-incision and post-incision steps. In this paper, we compared the spatio-temporal distribution of RPA, RFC and PCNA, using immunofluorescence and live cell microscopy of the GFP-tagged versions of the three replication proteins, to uncover the dynamic interactions of these factors with the DNA template in different maintenance processes.

2. Materials and methods

2.1. Cell culture and transfection

All cell lines were cultured under standard conditions at 37 °C and 5% CO_2 in a humidified incubator. U2OS cells and SV40-immortilized MRC5 cells were grown in a 1:1 mixture of Ham's F10 and DMEM (Lonza), supplemented with 10% fetal calf serum (FCS) and 1% penicillin-streptomycin (PS). Human primary wild-type control fibroblasts (C5RO) and XPF deficient fibroblasts (XP51RO) were cultured in Ham's F10 supplemented with 15% FCS and 1% PS. C5RO and XP51RO cells were grown to confluence and then incubated for 5 days with medium containing 0.5% FCS to induce quiescence.

A retroviral plasmid encoding RPA70-GFP was stably expressed in U2OS, SV40-immortilized MRC5, C5RO and XP51RO cells. Additionally, a cDNA encoding GFP-PCNA was stably expressed either by retroviral infection in C5RO hTERT [20] or by transfection [21] in SV40 immortalized MRC5. Cell lines expressing other fluorescent tagged proteins were used as described previously: RFC140-GFP [22], XPC-GFP [23] and GFP-XPA [24].

30 min before irradiation cells were treated with 100 mM hydroxyurea and 10 μM cytosine-β-arabinofuranoside to inhibit DNA synthesis. For global and local UV irradiation cells were washed with PBS and subsequently exposed to a UV-C germicidal lamp (254 nm, Philips) at the indicated dose [25]. To apply local UV damage cells were UV irradiated through an isopore membrane filter (Millipore), containing 5 μm pores.

2.2. Western blotting

For western blotting, primary mouse antibodies against RPA (B-6/sc-28304, Santa Cruz Biotechnology, Inc.) and GFP (11 814 460 001, Roche) were used in combination with Alexa Fluor 795 donkey anti-mouse antibodies (LI-COR). Antibody complexes were visualized using the Odyssey CLx Infrared Imaging System (LI-COR Biosciences).

2.3. Immunofluorescence

Cells were fixed using 2% paraformaldehyde supplemented with 0.1% Triton X-100. Samples were processed as described previously [24]. For GFP staining, cells were permeabilized with 0.5% Triton X-100 for 30 s prior to fixation. The following primary antibodies were used: anti-Ki67 (Ab833, Abcam), anti-XPC [26], anti-TFIIH p89 (s-19, Santa Cruz Biotechnology), anti-6-4pp (64M-2, Cosmo Bio), anti-RPA32 (ab2175, Abcam), anti-GFP (ab290, Abcam) and combined with secondary antibodies labeled with ALEXA fluorochromes 488 or 594 (Invitrogen; The Jackson Laboratory) for visualization. Samples were finally embedded in DAPI vectashield (Vector Laboratories). Anti-XPA (FL-273, Santa Cruz Biotechnology) or mouse anti-CPD (TDM-2, MBL International) was used as marker of local UV damage, depending on the species in which the other antibody was raised. Colocalization was defined as an >2 fold increase in fluorescent intensity at the LUD and quantified by counting at least 40 cells. Edu (5-ethynyl-2′-deoxyuridine) incorporation was visualized using Click-iT Alexa Fluor 647 according to the manufacturer's protocol (Invitrogen). Optical images were obtained using a Zeiss LSM 510 META confocal microscope equipped with 63 × oil Plan-Apochromat 1.4 NA oil immersion lens (Carl Zeiss Inc.) and a pinhole aperture setting of 2.0 airy units.

2.4. Live cell confocal laser-scanning microscopy

Confocal laser scanning microscopy images were obtained using a Zeiss LSM 510 microscope equipped with a 25 mW Argon laser (488 and 561 nm) and 63 × oil Plan-Apochromat 1.4 NA oil immersion lens (Carl Zeiss Inc.).

Kinetic studies of GFP-tagged RPA, PCNA, RFC, XPC and XPA accumulation were executed as described previously [27]. Cells were grown in glass bottom dishes (MatTek, Ashland, MA, USA) and irradiated with a UV-C source containing four UV lamps (Philips TUV 9W PL-S) above the microscope stage. For induction of local damage, cells were UV-irradiated through a polycarbonate mask (Millipore Billerica, Massachusetts, USA) with pores of 5 μm and subsequently irradiated for 39 s (100 J/m^2) [28,29] and monitored for up to 5 h. Fluorescence intensity was normalized between 0 and 100%. Assembly kinetics were measured on a Zeiss Axiovert 200 M wide field fluorescence microscope, equipped with a 100x Plan-Apochromat (1.4 NA) oil immersion lens (Zeiss, Oberkochen, Germany), a Cairn Xenon Arc lamp with monochromator (Cairn research, Kent, U.K.) and an objective heater and climate chamber. Images were recorded with a cooled CCD camera (Coolsnap HQ, Roper Scientific, USA) using Metamorph 6.1 imaging software (Molecular devices, Downingtown, PA, USA). Cells were examined in microscopy medium (137 mM NaCl, 5.4 mM KCl, 1,8 mM $CaCl_2$, 0.8 mM $MgSO_4$, 20 mM D-glucose and 20 mM HEPES) at 37 °C.

To determine protein mobility FRAP was performed as described [30]. Indicated areas were photobleached by two iterations using 100% 488 nm laser power. The recovery of fluorescence in the photobleached area was monitored for the indicated times. Data was normalized to the overall fluorescence of the cell before bleaching.

Half nucleus bleaching combined with FLIP-FRAP was performed as described previously [22]. Half of the nucleus was bleached and subsequently the fluorescence recovery in the bleached area and the loss of fluorescence in the non-bleached area was measured for up to 4 min. For data analysis the difference in fluorescence signal between FLIP and FRAP before bleaching was set at 0 and the difference between FLIP and FRAP after bleaching

was normalized to 1. The mobility of a protein was determined as the time necessary for FLIP-FRAP to return to 0.

FLIP analysis was performed by continuously photobleaching a third of a locally-irradiated nucleus opposite to the site of damage with 100% 488 nm laser intensity, as described previously [27,29,31]. Fluorescence in the locally irradiated area was monitored with normal laser intensity until fluorescence was completely lost. All values were background corrected.

3. Results

3.1. Differential nuclear localization of RFC140, PCNA and RPA70 during the cell cycle

To study the spatio-temporal distribution of core DNA replication factors implicated in the DNA damage response (DDR) we first analyzed the localization of RPA, RFC and PCNA in unperturbed living cells. We used cell lines that stably express GFP-tagged RFC [22] and PCNA [32] and generated cells that stably express RPA70-GFP. Immunoblot analysis showed that full-length RPA70-GFP is expressed at physiological levels (Fig. 1A). RPA70-GFP shows a homogeneous nuclear distribution, with lower expression in nucleoli in addition to a varying number of sub-nuclear structures with higher local concentrations. This distribution pattern is similar to endogenous RPA as shown by immunofluorescence (Fig. 1B). Sub-nuclear structures with higher local concentrations were independent of the cell cycle phase and were previously described to co-localize with promyelocytic leukemia (PML) body markers [33,34].

Within an asynchronously growing cell population we observed, in approximately 40% of the cells expressing RFC140-GFP and GFP-PCNA, the typical S-phase focal distribution (Fig. 1C) [22,35]. Interestingly, in contrast to these factors, the typical 'replication foci' were not observed in RPA70-GFP expressing cells. To verify that the absence of replication foci in these cells was not due to the imaging conditions or to a strong reduction in the relative number of S-phase cells, we investigated the cell cycle dependent distribution of RPA70-GFP in cells coexpressing mCherry-PCNA to identify cells in S-phase [36]. We observed no focal accumulation of RPA70-GFP although these cells clearly showed mCherry-PCNA foci indicating that these cells were in S-phase (Fig. 1D). Thus far RPA-foci in S-phase cells could only be detected in fixed cells, using antibodies directed against endogenous RPA [37]. These data suggest that RPA, although an essential replication factor, is not visibly clustered into replication foci in living cells. In line with our observations, the *in vivo* localization GFP-RPA32, was previously investigated and also no replication foci of this RPA subunit were observed in living S-phase cells [38,39].

3.2. GFP-PCNA, RPA70-GFP and RFC140-GFP mobility

Despite the proven involvement of PCNA, RFC and RPA in replication [40], RPA does not cluster in replication foci. This apparent discrepancy in subcellular localization may be explained by their different binding times. Previous FRAP studies have shown that in non-S-phase cells the mobility of GFP-PCNA and RFC140-GFP is mainly determined by free diffusion [21,22]. To compare the dynamic properties of these two proteins with those of RPA in living cells, we applied an adapted FRAP procedure, designated FLIP-FRAP. This procedure is specifically suited to determine subtle differences in overall nuclear mobility [31]. The mobility curves of GFP-PCNA and RPA70-GFP in non-S-phase cells were comparable (Fig. 2A), with a half-life of approximately 7.5 s. RFC140-GFP showed a much longer half-life of approximately 30 s (Fig. 2A). The slower diffusion of RFC140-GFP is likely related to the molecular shape and size of the RFC complex, which is almost twice the molecular weight of either the PCNA trimer or the RPA hetero-trimer. Although the mobilities of PCNA and RPA appeared very similar in non-S-phase cells, a striking difference was observed in S-phase cells (Fig. 2B). As expected from earlier studies [21,41], the mobility of GFP-PCNA during S-phase ($t_{1/2}$ = 40 s) was significantly slower than in non-S-phase cells ($t_{1/2}$ = 7.5 s), which is most likely caused by a relatively long PCNA binding in replication factories. Interestingly, the dynamics of RPA70-GFP in non-S-phase cells was similar to that determined in S-phase cells. The striking differences in the mobility between PCNA ($t_{1/2}$ = 40 s) and RPA ($t_{1/2}$ = 7.5 s) in S-phase are most likely explained by the very short binding time of RPA70-GFP molecules to DNA replication substrates and/or factors, while PCNA is bound significantly longer. This suggested transient association would also explain the lack of clearly visible RPA70-GFP replication foci in S-phase cells in live-cell imaging experiments.

3.3. RPA is immobilized at HU/AraC inhibited replication forks

To investigate whether the dynamic association of RPA70-GFP in replication foci is indeed too transient to be visualized using live cell imaging, we attempted to slow-down its DNA binding kinetics by inhibiting DNA synthesis using hydroxyurea (HU) and cytosine-β-arabinofuranoside (AraC). Upon treatment, a large number of cells exhibited clear S-phase foci (Fig. 2C), indicating that RPA70-GFP protein is biologically active and capable of binding at replication sites. This observation is in line with previous reports, which also showed pronounced focal localization of RPA32-GFP upon treatment of cells with the DNA polymerase-inhibitor, aphidicolin [38].

The presence of RPA70 at replication foci upon replication inhibition might be explained by an increased amount of substrate or an increased binding time of RPA to ssDNA. Therefore, we measured the mobility of RPA70-GFP by photobleaching upon replication inhibition by HU and AraC. A small square within nuclei was photo-bleached and the subsequent recovery of fluorescence, which reflects the effective diffusion rate, was monitored (Fig. 2D). Inhibition of replication fork progression induces an overall slower mobility of RPA70-GFP in the nucleus, likely caused by the transient immobilization of a fraction of RPA molecules at inhibited replication forks. Interestingly, our data suggest that during normal replication the coating of ssDNA with RPA is a highly dynamic process in which individual RPA molecules swiftly bind to and dissociate from its substrate most probably mediated by active DNA polymerases.

3.4. RPA70-GFP accumulates for up to 8 h at sites of local UV damage

RPA, PCNA and RFC are not solely involved in DNA replication but also in several DNA repair processes such as NER. In order to obtain information on the dynamic interactions of these replication factors with DNA damage, we determined the assembly kinetics of RPA and RFC and compared it with the previously determined kinetics of PCNA as well as that of the pre-incision NER factors, XPC and XPA [27]. Accumulation of NER factors at sites of local UV damage (LUD) was investigated in a population of asynchronous living cells expressing the fluorescent tagged versions of these proteins. The DNA damage-recognition factor XPC started to accumulate at sites of LUD immediately after DNA damage infliction. For the down-stream pre-incision factor XPA a slight delay in accumulation was observed. As RPA is present at the same pre-incision step during NER as XPA [42,43], similar accumulation kinetics were expected. However RPA accumulation was slower than that of XPA. RPA reached a maximum accumulation after 200 min, resembling the accumulation kinetics of the repair replication factors PCNA

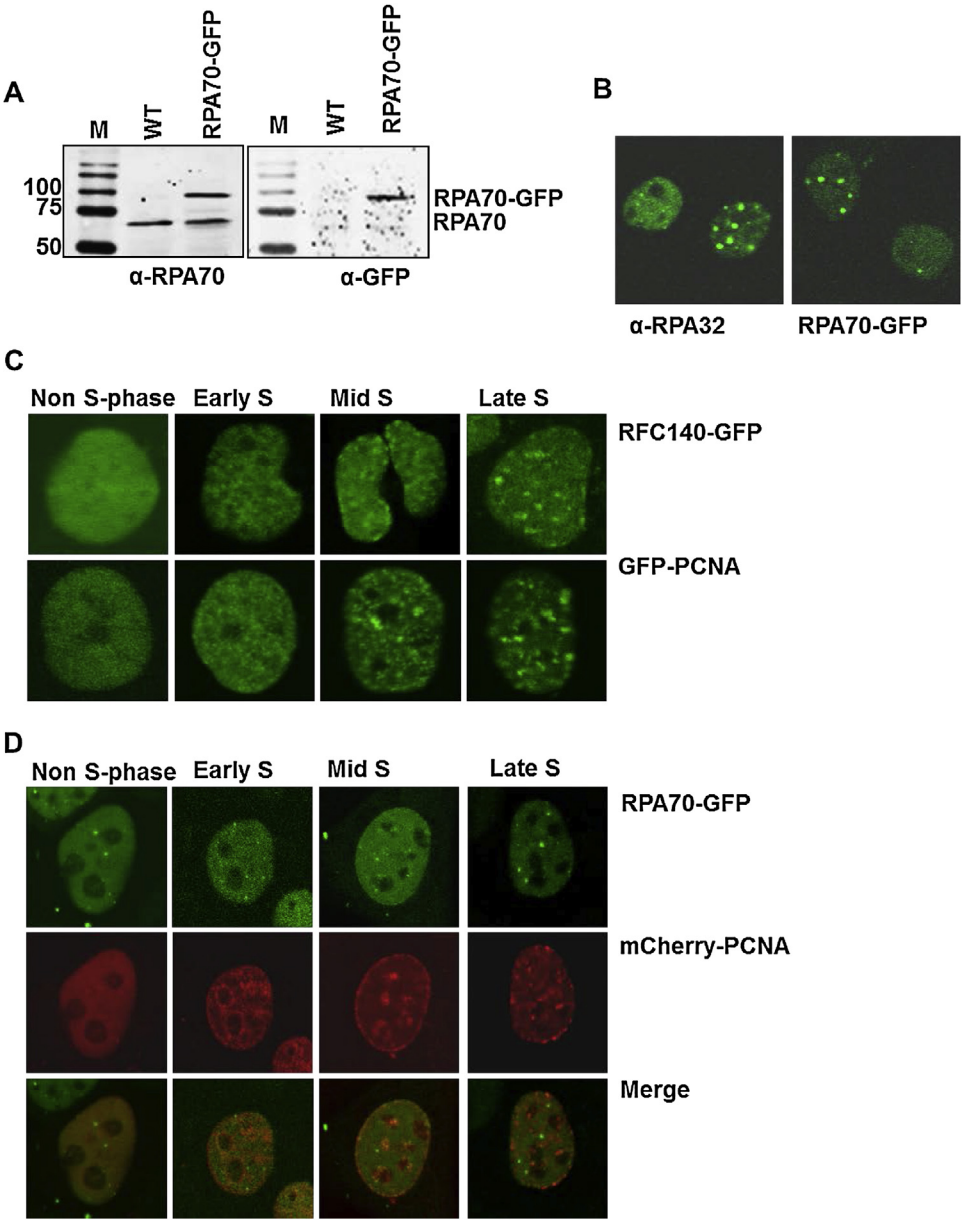

Fig. 1. Characterization and subcellular localization of RPA70-GFP. (A) Comparison of the RPA70-GFP and the endogenous RPA70 protein levels. Equal amounts of lysates of U2OS cells stably expressing RPA70-GFP and WT U2OS cells were immunoblotted and probed with antibodies against RPA70 and GFP. The protein marker is indicated with M. The expression levels of RPA70-GFP and endogenous RPA70 are comparable. Experiment was performed twice. (B) A representative image of a comparison of RPA localization in fixed U2OS cells (left) and U2OS cells stably expressing RPA70-GFP (right). Endogenous RPA was visualized in WT cells using an antibody specific for the RPA32 subunit. RPA70-GFP shows a similar nuclear distribution to endogenous RPA, with a lower expression in nucleoli and a higher expression in sub-nuclear foci. Experiment was performed at least four times. (C) Representative images of living MRC5 cells stably expressing RFC140-GFP and GFP-PCNA, experiment was performed twice. The replication factors display a homogenous localization in cells in G1 and G2 phase of the cell cycle but distinct focal patterns in specific stages of the S-phase. (D) Representative images of living MRC5 cells stably co-expressing RPA70-GFP and mCherry-PCNA. RPA70-GFP displays a similar localization throughout the cell cycle as defined by mCherry-PCNA as S-phase marker. Experiment was performed twice.

and RFC (Fig. 3A, supplemental Fig. 1). Although it is known that RPA functions in the pre-incision step of NER [44], these data suggest that the visible RPA accumulation is mainly derived from its function in the post-incision step of NER.

Accumulation of RPA at sites of LUD at later time points after UV irradiation may represent replication-stress in cells that were in S-phase at the moment of damage infliction or that entered this phase despite the presence of DNA damage, rather than reflecting its activity during the NER reaction. To further dissect this possibility, local UV irradiated cells were incubated with the thymidine analog EdU. Cells that were in S-phase during the experiment were detected by EdU incorporation. Accumulation of RPA at sites of LUD, using XPA as a damage marker, is visible in both S-phase and non S-phase cells (Fig. 3B). This suggests that RPA accumulation at sites of LUD reflects NER replication sites and is not solely caused by replication stress.

To confirm these observations we also studied the accumulation of RPA and other pre-incision NER factors, XPC and XPB in quiescent cells, where no replication processes occur, as shown by the absence of Ki-67 staining (Supplemental Fig. 2A). Cells were fixed at various time-points post UV irradiation (15 min, 30 min, 1 h and 2 h) and immunostained for 6-4PP, XPC, XPB and RPA. As expected, the pre-incision factors XPC and XPB accumulated at sites of LUD shortly after damage infliction (within 15 min) and started to disappear after 2 h following the removal of 6-4PP (Fig. 3C, supplemental Figs. 2B–D). In contrast, while only a faint RPA signal

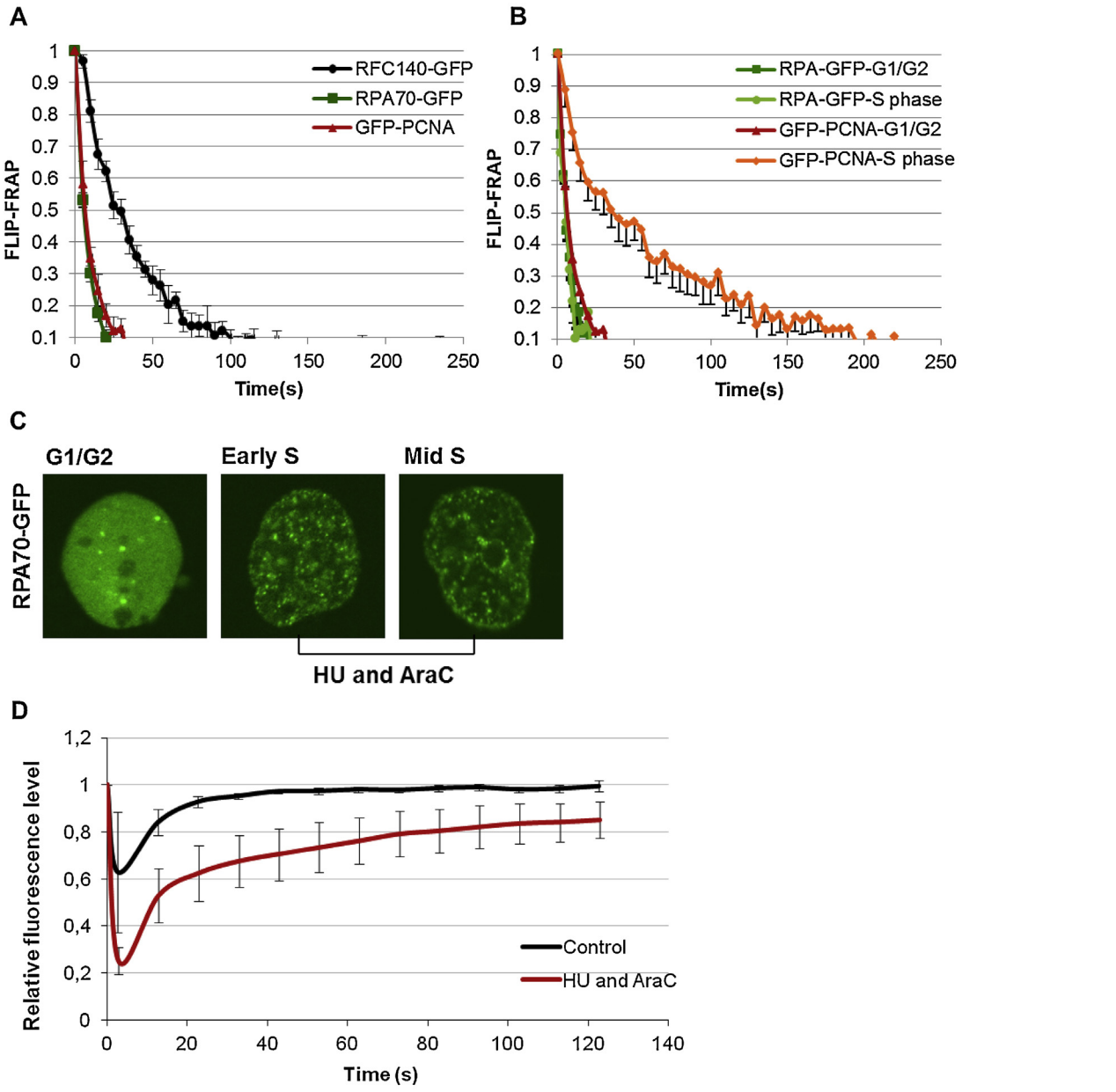

Fig. 2. Mobility of RPA70-GFP. (A) FLIP-FRAP analysis in untreated MRC5 cells expressing RFC140-GFP, C5RO cells expressing GFP-PCNA and MRC5 cells expressing RPA70-GFP (at least 8 cells were analyzed, mean ± SEM). Half of the nucleus was bleached with 100% laser power. The loss of fluorescence was measured (FLIP) in the unbleached area and recovery of fluorescence (FRAP) was monitored in the bleached area of the cell. The difference between FLIP and FRAP was normalized to 1 directly after the bleach pulse. The diffusion curves show that RFC140-GFP diffuses much slower than the other replication factors. (B) FLIP-FRAP analysis in MRC5 RPA70-GFP and C5RO GFP-PCNA in S-phase versus G1- or G2-phase cells ($N = 8$, mean ± SEM). GFP-PCNA is immobilized during S-phase, while RPA70-GFP kinetics is similar throughout the cell cycle. RPA70-GFP expressing MRC5 cells in S-phase were identified by co-expression of the S-phase marker mCherry-PCNA. (C) Representative pictures of living MRC5 RPA70-GFP cells that were exposed to HU and AraC for 30 min. In the presence of DNA synthesis inhibitors, RPA70-GFP is visible at replication foci. (D) Quantitative FRAP analysis on MRC5 cells stably expressing RPA70GFP in the presence and absence of the DNA synthesis inhibitors HU and AraC. The fluorescence in a small square within the nucleus was bleached and the fluorescence recovery was measured and normalized to pre-bleach intensity ($N = 5$, mean ± SEM).

could be detected at sites of LUD at the earliest time point (15 min), a stronger signal was detected at 1 h after UV and remained visible up to 8 h post UV irradiation (Fig. 3C and D). These data suggest that the long-lasting accumulation of RPA is related to post-incision events of NER and is not solely caused by stalled replication forks at sites of UV-damage.

3.5. Dynamics of RPA70-GFP in the pre- and post-incision steps of NER

As shown above, RPA can be visualized at sites of LUD at later time points post-UV relative to other pre-incision NER factors, despite the fact that it is absolutely required during the pre-incision-step [44,45]. This late accumulation at sites of LUD suggests that the binding time of RPA in the pre-incision NER step is too short to result in detectable accumulation at sites of LUD, which is in line with the observation that RPA is not visible at replication foci (Fig. 1D). To reveal RPA binding to pre-incision NER intermediates we made use of a specific XPF mutant cell line, XP51RO. Due to a missense mutation in XPF this endonuclease is mis-localized in the cytoplasm and therefore cannot execute the essential 5′ incision during NER [46]. Since these XP-F cells are devoid of dual incision events, no post-incision repair replication associated RPA accumulation is expected.

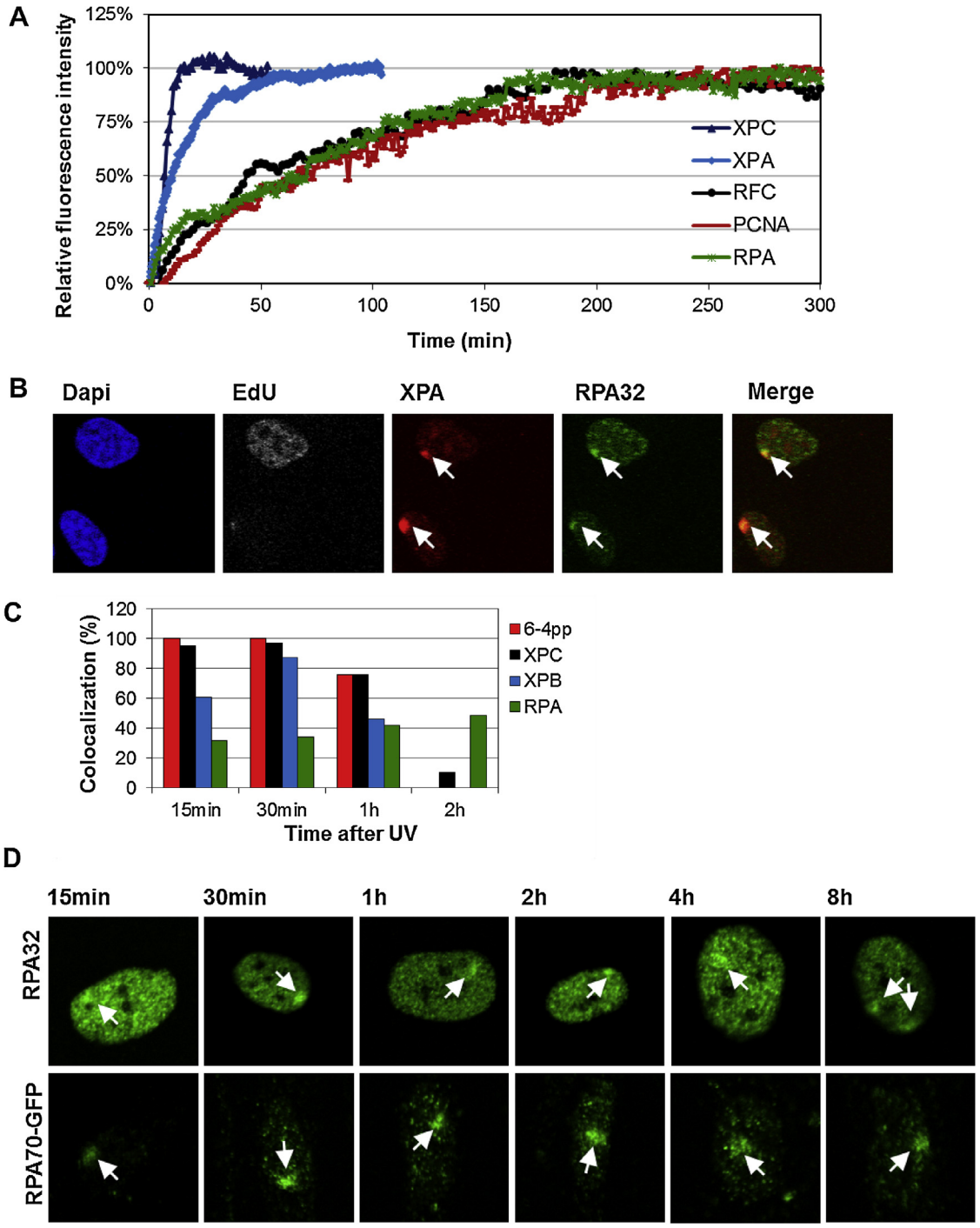

Fig. 3. Accumulation kinetics of pre- and post-incision factors at sites of local UV damage. (A) Cells stably expressing XPC-GFP ($N = 12$), GFP-XPA ($N = 7$), RFC140-GFP ($N = 7$), GFP-PCNA ($N = 5$) and RPA70-GFP ($N = 5$) were locally UV irradiated (100 J/m^2) through 5 μm diameter pores. GFP fluorescence intensities at the site of UV damage were measured by real time imaging until a maximum was reached. Relative fluorescence was normalized to 0 (before damage) and 100% (maximum level of fluorescence). (B) U2OS cells were exposed to local UV damage (60 J/m^2) and directly after damage incubated for 30 min in medium containing EdU. S-phase cells were identified by EdU incorporation, visualized by Alexa 647. Cells were immunostained for RPA32 and XPA. RPA accumulates at LUD in both S-phase and non-S-phase cells. Arrows indicate local damage. Experiment was performed twice. (C) Quantification of co-localization of the indicated proteins at LUD with a damage marker at various time points after local UV irradiation (40 J/m^2). XPA was used as damage marker for 6-4PP and RPA stainings, whereas CPD was used as damage marker for XPC and XPB stainings. Co-localization was defined as ≥2-fold increase in intensity at LUD and analyzed in 40 cells, experiment was performed twice. (D) Representative pictures of RPA in locally UV irradiated (40 J/m^2) quiescent C5RO cells visualized with anti-RPA32 and quiescent C5RO cells stably expressing RPA70-GFP. RPA is visible at the site of damage up to 8 h after UV. Arrows indicate LUD. Experiment was performed twice.

Despite the absence of incision, colocalization of RPA32 to sites of LUD was higher in XPF mutant cells than in wild type cells at all time points (Fig. 4A). In addition, RPA signal-intensity at sites of LUD was higher in XP-F cells. Similar results were observed for the GFP-tagged version of RPA70 (Supplemental Fig. 3). Thus, due to the absence of ERCC1/XPF mediated incision, the stronger RPA signal at LUD could be explained by an extended lifetime and/or an increased number of unwound and RPA coated pre-incision NER-intermediates. To determine the dynamic association of RPA in non-processed pre-incision NER complexes, we compared, using

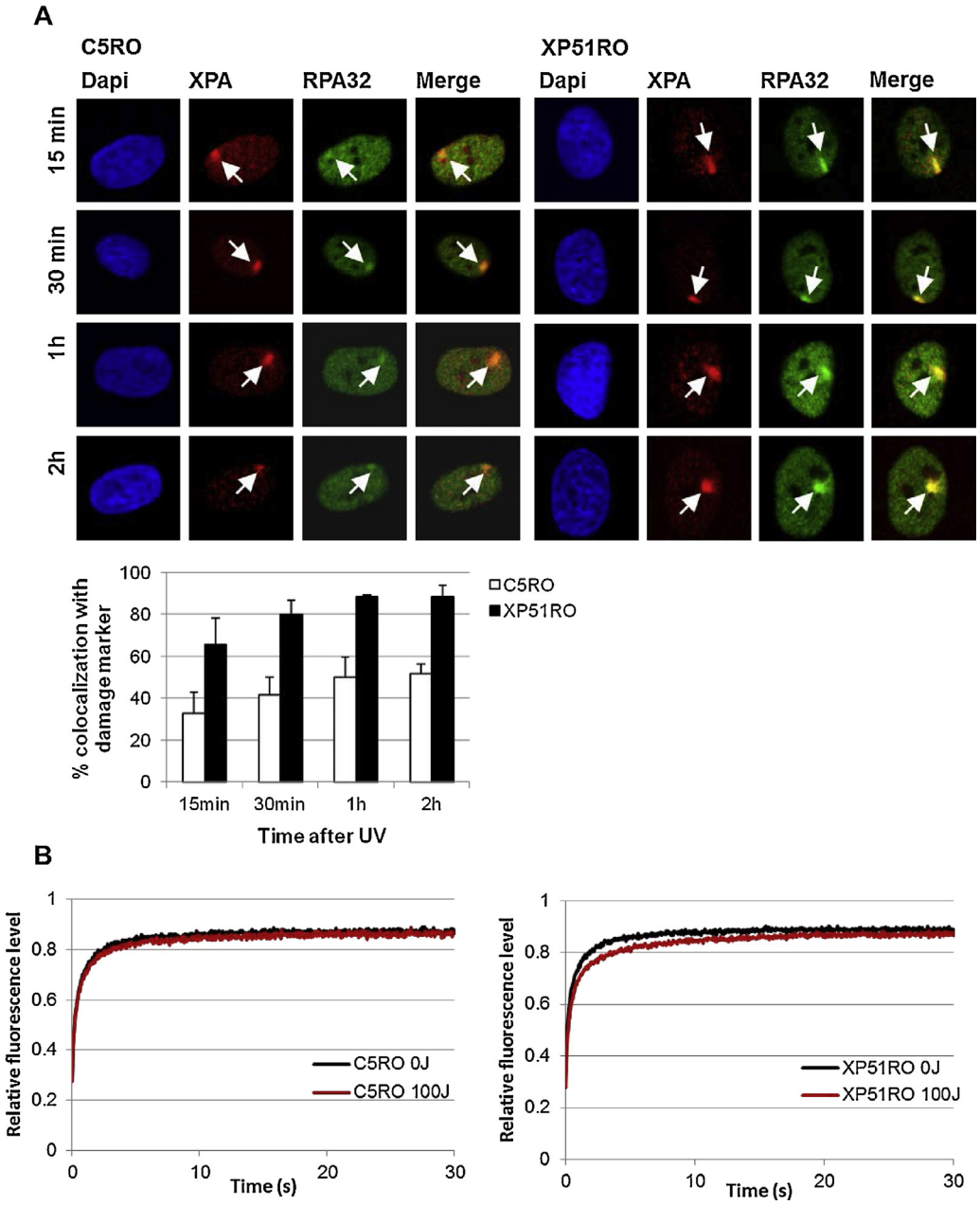

Fig. 4. Dynamics of RPA in XPF deficient cells. (A) Quiescent C5RO and XP51RO (XPF deficient) cells were local UV irradiated (40 J/m^2). Cells were fixed at the indicated time points after UV and immunostained for RPA32 and XPA. Arrows indicate local damage sites. The percentage of colocalization of RPA32 with XPA after LUD is plotted in the graph. At least 40 cells with LUD were analyzed in three independent experiments (mean ± SD). (B) FRAP analysis of RPA70-GFP in non-damaged and global UV irradiated (100 J/m^2) C5RO and XP51RO (XPF deficient) cells. FRAP was performed directly after UV treatment. The recovery was normalized to pre-bleach intensity (N = 24, from two independent experiments).

FRAP, the mobility of RPA70-GFP, in UV-irradiated XP-F and wild-type cells. In XPF mutant cells, we observed a small transient immobilization of RPA70-GFP upon UV damage, which was not present in wild-type cells (Fig. 4B). This difference however, is most likely too small to account for the increased signal of RPA in XP-F cells. Probably XP-F cells accumulate more pre-incision NER intermediates (RPA substrates) at any given time, resulting in a higher RPA signal. Together these data show that RPA displays a remarkable highly dynamic association with DNA during the assembly of the pre-incision NER complex. The binding kinetics are that short that they could not be revealed under standard live-cell imaging conditions in NER proficient cell lines.

In contrast to other pre-incision factors, but similarly to RFC, RPA is present for a prolonged time at sites of DNA damage [22]. This different kinetic behavior is probably derived from its function in the post-incision steps of NER. To further decipher the mode of action of RPA70-GFP during the post-incision steps of NER, we used the DNA synthesis inhibitors HU/AraC. Upon treatment with HU/AraC, repair associated DNA synthesis is inhibited and NER induced ssDNA remains, which represents post-incision intermediates [22]. Under these conditions it is possible to study RPA kinetics specifically at the post-incision steps of NER. Cells were treated with HU/AraC or mock treated 30 min prior to LUD infliction, and fixed 1 h later. During the entire procedure cells were cultured in the presence of EdU. UV-irradiated areas were visualized using CPD immunostaining. In response to an UV dose of 30 J/m^2 RPA70-GFP accumulation is not detectable at sites of LUD, independent of the cell cycle phase (Fig. 5A, Top panel). Note that

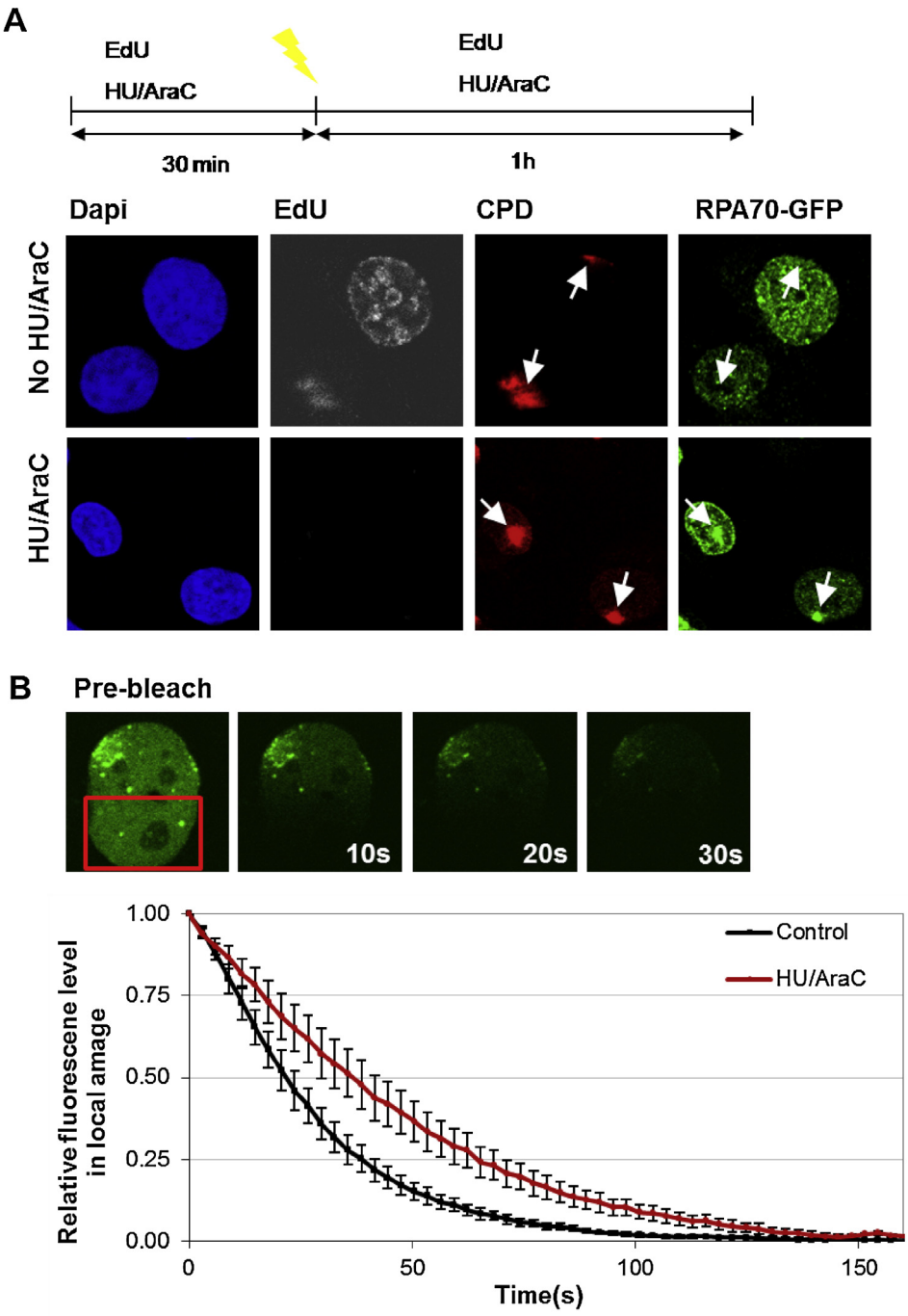

Fig. 5. Dynamics of RPA70-GFP at sites of LUD upon HU/AraC treatment. (A) A representative image of RPA70-GFP expressing U2OS cells that were mock treated or incubated with HU and AraC for 30 min before local UV irradiation (30 J/m^2). Cells were fixed 1 h after UV exposure. S-phase cells were identified by EdU incorporation, visualized by Alexa647 or by localization of RPA70-GFP. The UV-irradiated areas were visualized using an antibody specific for CPDs. In the presence of DNA synthesis inhibitors RPA70-GFP accumulation is visible at LUD in both S-phase and non-S-phase cells. Arrows indicate local damage. Experiment was performed twice. (B) Dissociation kinetics of RPA70-GFP from LUD in mock or HU and AraC treated cells (30 min). MRC5 RPA70-GFP cells were locally UV irradiated (100 J/m^2) and one third of the nucleus was continuously bleached. The decrease of fluorescence in the LUD was quantified ($N \geq 12$, from two independent experiments; mean ± SEM). The residence time of RPA70-GFP at LUD is longer in cells treated with DNA synthesis inhibitors.

in the non-replicating cell the DNA repair replication is active as shown by the EdU incorporation at LUD. Despite this clear mark of DNA synthesis, under these conditions no local RPA accumulation is visible. However, when DNA synthesis was blocked with HU and AraC, as shown by the lack of EdU incorporation, RPA70-GFP accumulation at sites of LUD was clearly detected (Fig. 5A, Lower panel). The same was observed for the endogenous protein visualized using an antibody against RPA32 (Supplementary Fig. 4). This could be explained either by an increase in the number of binding sites for RPA or by a more stable association of RPA with ssDNA.

To gain more insight into the dynamic association of RPA with sites of HU/AraC-inhibited repair replication, we performed a FLIP experiment at sites of LUD to measure the off-rate of RPA from sites of DNA damage. 1 h after local UV irradiation, an area in the nucleus representing approximately one third of the nuclear

volume located opposite of the LUD was continuously bleached. The intensity of fluorescence in the local damage was measured [47]. The time it takes to lose the fluorescent signal at LUD by this procedure is a measurement for the dissociation rate of the RPA-GFP molecules. The average binding time of RPA70-GFP molecules was longer (~2-fold) in the presence of inhibitors than in cells with processive DNA repair synthesis (Fig. 5B), suggesting that the DNA polymerases involved in DNA repair synthesis have an important impact on the residence time of RPA at the ssDNA gap. In summary these data demonstrate that RPA presents differential kinetic properties in pre- and post-incision steps of NER.

4. Discussion

4.1. Dynamics at replication sites

The DNA synthesis step of DNA replication of the genome requires the concerted action of many proteins including: DNA polymerases, the polymerase clamp (PCNA), the clamp loading complex (RFC), and the single-stranded DNA-binding protein complex (RPA) [40]. Replication factors, such as PCNA and RFC show specific distribution patterns throughout the S-phase known as replication foci or replisomes (Fig. 1C) [35]. In line with this, PCNA and RFC become less mobile during S-phase compared to G1 or G2 phases of the cell cycle (Fig. 2B) [21]. Interestingly, and in contrast to PCNA and RFC, the 2 largest subunits of replication protein A (RPA70 and RPA32) are not visible in replication foci in living cells (Fig. 1D) [38,41]. Thus far, RPA has only been detected in replication foci upon fixation followed by immunofluorescence [37]. In this procedure the bound RPA at sites of replication is fixed and unbound RPA is most likely washed away enabling detection under such conditions. However in living cells RPA does not visibly accumulate in replication foci, despite its established role in this process, which is likely due to the fast turnover of RPA molecules at replication sites. The dwell time of RPA at replication sites is in the same order of its respective diffusion rate (Fig. 2B), indicating that the ssDNA-RPA interaction is too transient to induce RPA steady-state levels above background.

DNA synthesis inhibitors such as HU and AraC have been shown to block DNA polymerases at replication forks, resulting in an increase of ssDNA patches [48], which are coated by RPA. Under these conditions, RPA accumulates in replication foci (Fig. 2C), indicating that RPA70-GFP is functional and binds at sites of replication. Similar results have been observed for GFP-RPA32 in cells treated with the DNA synthesis inhibitor aphidicolin [38,39]. DNA synthesis inhibition results in an excess of ssDNA [48], thereby increasing the amount of RPA-binding substrates, which partially explains the clear presence of RPA at sites of blocked replication. In addition, RPA mobility is greatly reduced upon inhibition of the DNA polymerases (Fig. 2D). These data further corroborate that although RPA coats ssDNA at sites of replication, it is not visible at replication foci in living cells in unperturbed conditions because it is swiftly displaced by the elongating DNA polymerases during replication [49]. It is however important to note that even when RPA is bound at the ssDNA patches induced by a replication block, it still binds transiently, indicating that it is an intrinsic property of RPA to continuously associate and dissociate from ssDNA, independently of DNA polymerases. These results are in line with the rapid RPA turnover on ssDNA *in vitro* [50]. In contrast to RPA, PCNA binds more stably at replication forks, most likely remaining at the site of replication until replication is completed [41]. This difference in residence time at the replication fork between RPA and PCNA likely explains why PCNA can be observed at replication sites in living cells, while RPA cannot.

4.2. RPA promotes two mechanistically distinct steps in NER

RPA plays a key role in the pre- as well as post-incision steps of NER. Intriguingly, while RPA binding kinetics is similar to the assembly kinetics of the replication factors PCNA and RFC, they are very different to those of the pre-incision NER factors XPC, XPB and XPA. Pre-incision factors accumulate rapidly after UV irradiation and their bound steady-state levels decrease within 2 h (Fig. 3C, supplemental Figs. 2B–D) [27], closely following the repair kinetics of 6-4 photoproducts. Conversely, RPA reaches it maximum only after 3 h and is still visible up to 8 h at sites of local UV damage (Fig. 3A and D).

Treatment of cells with DNA synthesis inhibitors, which also disturbs DNA synthesis during the gap-filling stage of NER, resulted in a more abundant accumulation of RPA at sites of DNA damage, which is likely due to longer residence times on the chromatin (Fig. 5B). On the contrary, the residence time of the pre-incision factors XPA and ERCC1 is not retarded by inhibition of DNA synthesis [27]. This suggests that the observed localization of RPA at LUD is mainly derived from its function in repair synthesis during the post-incision step of NER. In line with our results, previous studies showed that inhibition of either the DNA repair synthesis or ligation step of NER, results in prolonged presence of RPA at sites of LUD, while other pre-incision factors are still able to dissociate and relocate to other damage sites [19]. While Overmeer et al. report that RPA remains bound at sites of DNA damage and does not relocate to engage new repair sites upon inhibition of DNA repair synthesis, our FRAP data clearly shows that, although its mobility is greatly reduced, RPA can still bind to and dissociate from the DNA continuously.

In XPF-deficient cells, incision does not take place and pre-incision NER intermediates accumulate [46]. These intermediates contain unwound DNA structures to which RPA binds. In these cells RPA accumulation at early time points was observed in a higher percentage of cells, more closely resembling the accumulation kinetics of other pre-incision factors. This demonstrates that although not clearly visible in repair proficient cells, RPA can be visualized in pre-incision NER intermediates. Interestingly, despite the accumulation of pre-incision NER-intermediates in XPF-deficient cells, RPA mobility was only minimally reduced, indicating that RPA binds to and dissociates from NER intermediates at almost similar rates to that in wild-type cells. This indicates that the rapid binding and dissociation of RPA in the pre-incision step of NER, just like during normal replication, is an intrinsic property of RPA. These data suggest that the binding time of RPA in the pre-incision steps of NER is too brief to be visualized in NER proficient cells.

The two major DNA lesions induced by UV irradiation display different repair kinetics: while local induced 6-4PPs are repaired (depending on the dose) within ~2 to 4 h; CPD repair is not achieved within 24 h [51]. Previous studies showed that accumulation of NER factors to LUD follow the repair kinetics of 6-4PP [27,51]. It is unlikely that RPA accumulation to LUD at late time points is due to repair of 6-4PPs. It is more probable that RPA is involved in other processes, for example those linked to the persistent presence of CPD lesions. It is possible that accumulation of RPA at late time points after UV is a result of replication stress due to replication fork stalling at UV lesions in cells that were in S-phase at the moment of damage infliction or that moved into this phase despite the presence of DNA damage. However RPA accumulation at late time points is also observed in non-S-phase cells (Fig. 3B) and quiescent cells, where no replication occurs (Fig. 3D). These results suggest that RPA accumulation to LUD at late time points marks post-incision NER sites. This hypothesis is supported by the fact that – like RPA – PCNA and RFC also localize to sites of LUD in quiescent cells up to 8 h post-irradiation [22].

Whether the ssDNA NER intermediates, formed by the joint action of the XPF/ERCC1 and XPG nucleases, are alone responsible for this long-lasting RPA accumulation at sites of damage is questionable; especially since NER intermediates are short ssDNA gaps (~30 nt long) which can, most likely, bind only one RPA trimer. Moreover, the ssDNA NER intermediates are likely very short lived, being rapidly refilled by DNA polymerases during DNA repair synthesis, which might take place even before incision 3′ to the UV lesion [15]. Recent studies have shown that the exonuclease activity of EXO1 is implicated in the processing of NER intermediates, thereby generating long stretches of ssDNA that are coated by RPA [52,53]. This can also happen in non-cycling cells under specific conditions that might occur when the normally short-lived ssDNA NER intermediates persist. Examples of such conditions are when the damage load in the cell is so high that the concentration of NER factors might become limiting, or during the collision of two opposing NER reactions when the opposing lesion is blocking the progression of NER-induced gap filling synthesis. Indeed, a possible explanation for the accumulation of RPA, PCNA and RFC at late time points after UV irradiation is that lesions that are difficult to repair are processed to long ssDNA gaps by the exonuclease activity of EXO1 to overcome these lesions. In line with this, others have shown that EXO1 accumulation is also increased at sites of DNA damage in situations where more RPA accumulates, for example upon inhibition of the gap-filling step of the NER reaction [53].

In summary, RPA displays differential dynamics during replication and at sites of NER. It binds ssDNA transiently during replication and the pre-incision steps of NER, but has a more stable association during the post-incision steps of NER and in response to replication stress. RPA is known to recruit ATR through its binding partner ATRIP in order to induce checkpoint activation and cell cycle arrest in response to both replication stress and UV damage [48]. If there are no obstacles during replication, RPA binding does not induce checkpoint activation. In line with this, studies in yeast have shown that very low doses of UV do not induce checkpoint activation [54]. We speculate that the differential dynamic behavior of RPA might be an important control factor for checkpoint activation. Binding of RPA during replication and pre-incision steps of NER is too transient to induce checkpoint activation, whereas the more stable association of RPA during replication stress and the post-incision steps of NER recruits ATR and ATRIP thereby activating a cellular response to cope with the damage.

Conflict of interest

None.

Acknowledgements

We would like to thank the optical imaging center (OIC) of the Erasmus MC for technical support on the microscopes. This work was funded by the Dutch Organization for Scientific Research ZonMW TOP Grant 912.08.031 and Horizon Zenith 93511042 (L.v.C. and W.V.), the Association for International Cancer Research 10-594 (M.T. and W.V.), ERC Advanced Grant 340988_ERC-ID to W.V, and a Veni Grant 917.96.120 and Erasmus MC fellowship (J.A.M).

Appendix A. Supplementary data

Supplementary data associated with this article can be found, in the online version, at http://dx.doi.org/10.1016/j.dnarep.2014.09.013.

References

[1] M.S. Wold, Replication protein A: a heterotrimeric, single-stranded DNA-binding protein required for eukaryotic DNA metabolism, Annu. Rev. Biochem. 66 (1997) 61–92.
[2] W.L. de Laat, E. Appeldoorn, K. Sugasawa, E. Weterings, N.G. Jaspers, J.H. Hoeijmakers, DNA-binding polarity of human replication protein A positions nucleases in nucleotide excision repair, Genes Dev. 12 (1998) 2598–2609.
[3] C. Iftode, Y. Daniely, J.A. Borowiec, Replication protein A (RPA): the eukaryotic SSB, Crit. Rev. Biochem. Mol. Biol. 34 (1999) 141–180.
[4] J. Majka, P.M. Burgers, The PCNA-RFC families of DNA clamps and clamp loaders, Prog. Nucleic Acid Res. Mol. Biol. 78 (2004) 227–260.
[5] G.L. Moldovan, B. Pfander, S. Jentsch, PCNA, the maestro of the replication fork, Cell 129 (2007) 665–679.
[6] R.T. O'Keefe, S.C. Henderson, D.L. Spector, Dynamic organization of DNA replication in mammalian cell nuclei: spatially and temporally defined replication of chromosome-specific alpha-satellite DNA sequences, J. Cell Biol. 116 (1992) 1095–1110.
[7] O.D. Scharer, Nucleotide excision repair in eukaryotes, Cold Spring Harb. Perspect. Biol. 5 (2013) a012609.
[8] K. Sugasawa, J.M. Ng, C. Masutani, S. Iwai, P.J. van der Spek, A.P. Eker, F. Hanaoka, D. Bootsma, J.H. Hoeijmakers, Xeroderma pigmentosum group C protein complex is the initiator of global genome nucleotide excision repair, Mol. Cell 2 (1998) 223–232.
[9] J. Moser, M. Volker, H. Kool, S. Alekseev, H. Vrieling, A. Yasui, A.A. van Zeeland, L.H. Mullenders, The UV-damaged DNA binding protein mediates efficient targeting of the nucleotide excision repair complex to UV-induced photo lesions, DNA Repair (Amst.) 4 (2005) 571–582.
[10] M. Fousteri, L.H. Mullenders, Transcription-coupled nucleotide excision repair in mammalian cells: molecular mechanisms and biological effects, Cell Res. 18 (2008) 73–84.
[11] W. Vermeulen, M. Fousteri, Mammalian transcription-coupled excision repair, Cold Spring Harb. Perspect. Biol. 5 (2013) a012625.
[12] M. Volker, M.J. Mone, P. Karmakar, A. van Hoffen, W. Schul, W. Vermeulen, J.H. Hoeijmakers, R. van Driel, A.A. van Zeeland, L.H. Mullenders, Sequential assembly of the nucleotide excision repair factors in vivo, Mol. Cell 8 (2001) 213–224.
[13] Z. He, L.A. Henricksen, M.S. Wold, C.J. Ingles, RPA involvement in the damage-recognition and incision steps of nucleotide excision repair, Nature 374 (1995) 566–569.
[14] T. Matsunaga, C.H. Park, T. Bessho, D. Mu, A. Sancar, Replication protein A confers structure-specific endonuclease activities to the XPF-ERCC1 and XPG subunits of human DNA repair excision nuclease, J. Biol. Chem. 271 (1996) 11047–11050.
[15] L. Staresincic, A.F. Fagbemi, J.H. Enzlin, A.M. Gourdin, N. Wijgers, I. Dunand-Sauthier, G. Giglia-Mari, S.G. Clarkson, W. Vermeulen, O.D. Scharer, Coordination of dual incision and repair synthesis in human nucleotide excision repair, EMBO J. 28 (2009) 1111–1120.
[16] J. Moser, H. Kool, I. Giakzidis, K. Caldecott, L.H. Mullenders, M.I. Fousteri, Sealing of chromosomal DNA nicks during nucleotide excision repair requires XRCC1 and DNA ligase III alpha in a cell-cycle-specific manner, Mol. Cell 27 (2007) 311–323.
[17] T. Riedl, F. Hanaoka, J.M. Egly, The comings and goings of nucleotide excision repair factors on damaged DNA, EMBO J. 22 (2003) 5293–5303.
[18] T. Ogi, S. Limsirichaikul, R.M. Overmeer, M. Volker, K. Takenaka, R. Cloney, Y. Nakazawa, A. Niimi, Y. Miki, N.G. Jaspers, et al., Three DNA polymerases, recruited by different mechanisms, carry out NER repair synthesis in human cells, Mol. Cell 37 (2010) 714–727.
[19] R.M. Overmeer, J. Moser, M. Volker, H. Kool, A.E. Tomkinson, A.A. van Zeeland, L.H. Mullenders, M. Fousteri, Replication protein A safeguards genome integrity by controlling NER incision events, J. Cell Biol. 192 (2011) 401–415.
[20] L.R. van Veelen, T. Cervelli, M.W. van de Rakt, A.F. Theil, J. Essers, R. Kanaar, Analysis of ionizing radiation-induced foci of DNA damage repair proteins, Mutat. Res. 574 (2005) 22–33.
[21] J. Essers, A.F. Theil, C. Baldeyron, W.A. van Cappellen, A.B. Houtsmuller, R. Kanaar, W. Vermeulen, Nuclear dynamics of PCNA in DNA replication and repair, Mol. Cell. Biol. 25 (2005) 9350–9359.
[22] R.M. Overmeer, A.M. Gourdin, A. Giglia-Mari, H. Kool, A.B. Houtsmuller, G. Siegal, M.I. Fousteri, L.H. Mullenders, W. Vermeulen, Replication factor C recruits DNA polymerase delta to sites of nucleotide excision repair but is not required for PCNA recruitment, Mol. Cell. Biol. 30 (2010) 4828–4839.
[23] D. Hoogstraten, S. Bergink, J.M. Ng, V.H. Verbiest, M.S. Luijsterburg, B. Geverts, A. Raams, C. Dinant, J.H. Hoeijmakers, W. Vermeulen, et al., Versatile DNA damage detection by the global genome nucleotide excision repair protein XPC, J. Cell Sci. 121 (2008) 2850–2859.
[24] S. Rademakers, M. Volker, D. Hoogstraten, A.L. Nigg, M.J. Mone, A.A. Van Zeeland, J.H. Hoeijmakers, A.B. Houtsmuller, W. Vermeulen, Xeroderma pigmentosum group A protein loads as a separate factor onto DNA lesions, Mol. Cell. Biol. 23 (2003) 5755–5767.
[25] M.J. Mone, M. Volker, O. Nikaido, L.H. Mullenders, A.A. van Zeeland, P.J. Verschure, E.M. Manders, R. van Driel, Local UV-induced DNA damage in cell nuclei results in local transcription inhibition, EMBO Rep. 2 (2001) 1013–1017.
[26] J.M. Ng, W. Vermeulen, G.T. van der Horst, S. Bergink, K. Sugasawa, H. Vrieling, J.H. Hoeijmakers, A novel regulation mechanism of DNA repair by damage-induced and RAD23-dependent stabilization of xeroderma pigmentosum group C protein, Genes Dev. 17 (2003) 1630–1645.

[27] M.S. Luijsterburg, G. von Bornstaedt, A.M. Gourdin, A.Z. Politi, M.J. Mone, D.O. Warmerdam, J. Goedhart, W. Vermeulen, R. van Driel, T. Hofer, Stochastic and reversible assembly of a multiprotein DNA repair complex ensures accurate target site recognition and efficient repair, J. Cell Biol. 189 (2010) 445–463.
[28] M.J. Mone, T. Bernas, C. Dinant, F.A. Goedvree, E.M. Manders, M. Volker, A.B. Houtsmuller, J.H. Hoeijmakers, W. Vermeulen, R. van Driel, In vivo dynamics of chromatin-associated complex formation in mammalian nucleotide excision repair, Proc. Natl. Acad. Sci. U. S. A. 101 (2004) 15933–15937.
[29] M.S. Luijsterburg, J. Goedhart, J. Moser, H. Kool, B. Geverts, A.B. Houtsmuller, L.H. Mullenders, W. Vermeulen, R. van Driel, Dynamic in vivo interaction of DDB2 E3 ubiquitin ligase with UV-damaged DNA is independent of damage-recognition protein XPC, J. Cell Sci. 120 (2007) 2706–2716.
[30] A.B. Houtsmuller, W. Vermeulen, Macromolecular dynamics in living cell nuclei revealed by fluorescence redistribution after photobleaching, Histochem. Cell Biol. 115 (2001) 13–21.
[31] D. Hoogstraten, A.L. Nigg, H. Heath, L.H. Mullenders, R. van Driel, J.H. Hoeijmakers, W. Vermeulen, A.B. Houtsmuller, Rapid switching of TFIIH between RNA polymerase I and II transcription and DNA repair in vivo, Mol. Cell 10 (2002) 1163–1174.
[32] S. Sabbioneda, A.M. Gourdin, C.M. Green, A. Zotter, G. Giglia-Mari, A. Houtsmuller, W. Vermeulen, A.R. Lehmann, Effect of proliferating cell nuclear antigen ubiquitination and chromatin structure on the dynamic properties of the Y-family DNA polymerases, Mol. Biol. Cell 19 (2008) 5193–5202.
[33] J. Park, T. Seo, H. Kim, J. Choe, Sumoylation of the novel protein hRIP{beta} is involved in replication protein A deposition in PML nuclear bodies, Mol. Cell. Biol. 25 (2005) 8202–8214.
[34] A. Groth, A. Corpet, A.J. Cook, D. Roche, J. Bartek, J. Lukas, G. Almouzni, Regulation of replication fork progression through histone supply and demand, Science 318 (2007) 1928–1931.
[35] S. Somanathan, T.M. Suchyna, A.J. Siegel, R. Berezney, Targeting of PCNA to sites of DNA replication in the mammalian cell nucleus, J. Cell. Biochem. 81 (2001) 56–67.
[36] G. Soria, L. Belluscio, W.A. van Cappellen, R. Kanaar, J. Essers, V. Gottifredi, DNA damage induced Pol eta recruitment takes place independently of the cell cycle phase, Cell Cycle 8 (2009) 3340–3348.
[37] K.G. Murti, D.C. He, B.R. Brinkley, R. Scott, S.H. Lee, Dynamics of human replication protein A subunit distribution and partitioning in the cell cycle, Exp. Cell Res. 223 (1996) 279–289.
[38] D.A. Solomon, M.C. Cardoso, E.S. Knudsen, Dynamic targeting of the replication machinery to sites of DNA damage, J. Cell Biol. 166 (2004) 455–463.
[39] S.M. Gorisch, A. Sporbert, J.H. Stear, I. Grunewald, D. Nowak, E. Warbrick, H. Leonhardt, M.C. Cardoso, Uncoupling the replication machinery: replication fork progression in the absence of processive DNA synthesis, Cell Cycle 7 (2008) 1983–1990.
[40] S. Waga, G. Bauer, B. Stillman, Reconstitution of complete SV40 DNA replication with purified replication factors, J. Biol. Chem. 269 (1994) 10923–10934.
[41] A. Sporbert, A. Gahl, R. Ankerhold, H. Leonhardt, M.C. Cardoso, DNA polymerase clamp shows little turnover at established replication sites but sequential de novo assembly at adjacent origin clusters, Mol. Cell 10 (2002) 1355–1365.
[42] L. Li, X. Lu, C.A. Peterson, R.J. Legerski, An interaction between the DNA repair factor XPA and replication protein A appears essential for nucleotide excision repair, Mol. Cell. Biol. 15 (1995) 5396–5402.
[43] E. Stigger, R. Drissi, S.H. Lee, Functional analysis of human replication protein A in nucleotide excision repair, J. Biol. Chem. 273 (1998) 9337–9343.
[44] D. Coverley, M.K. Kenny, M. Munn, W.D. Rupp, D.P. Lane, R.D. Wood, Requirement for the replication protein SSB in human DNA excision repair, Nature 349 (1991) 538–541.
[45] A. Aboussekhra, M. Biggerstaff, M.K. Shivji, J.A. Vilpo, V. Moncollin, V.N. Podust, M. Protic, U. Hubscher, J.M. Egly, R.D. Wood, Mammalian DNA nucleotide excision repair reconstituted with purified protein components, Cell 80 (1995) 859–868.
[46] A. Ahmad, J.H. Enzlin, N.R. Bhagwat, N. Wijgers, A. Raams, E. Appledoorn, A.F. Theil, J.H. JH., W. Vermeulen, J.J. NG., et al., Mislocalization of XPF-ERCC1 nuclease contributes to reduced DNA repair in XP-F patients, PLoS Genet. 6 (2010) e1000871.
[47] A. Pines, M.G. Vrouwe, J.A. Marteijn, D. Typas, M.S. Luijsterburg, M. Cansoy, P. Hensbergen, A. Deelder, A. de Groot, S. Matsumoto, et al., PARP1 promotes nucleotide excision repair through DDB2 stabilization and recruitment of ALC1, J. Cell Biol. 199 (2012) 235–249.
[48] L. Zou, S.J. Elledge, Sensing DNA damage through ATRIP recognition of RPA-ssDNA complexes, Science 300 (2003) 1542–1548.
[49] U. Hubscher, Y.S. Seo, Replication of the lagging strand: a concert of at least 23 polypeptides, Mol. Cells 12 (2001) 149–157.
[50] B. Gibb, L.F. Ye, Y. Kwon, H. Niu, P. Sung, E.C. Greene, Protein dynamics during presynaptic-complex assembly on individual single-stranded DNA molecules, Nat. Struct. Mol. Biol. 21 (2014) 893–900.
[51] J.A. Marteijn, S. Bekker-Jensen, N. Mailand, H. Lans, P. Schwertman, A.M. Gourdin, N.P. Dantuma, J. Lukas, W. Vermeulen, Nucleotide excision repair-induced H2A ubiquitination is dependent on MDC1 and RNF8 and reveals a universal DNA damage response, J. Cell Biol. 186 (2009) 835–847.
[52] M. Giannattasio, C. Follonier, H. Tourriere, F. Puddu, F. Lazzaro, P. Pasero, M. Lopes, P. Plevani, M. Muzi-Falconi, Exo1 competes with repair synthesis, converts NER intermediates to long ssDNA gaps, and promotes checkpoint activation, Mol. Cell 40 (2010) 50–62.
[53] S. Sertic, S. Pizzi, R. Cloney, A.R. Lehmann, F. Marini, P. Plevani, M. Muzi-Falconi, Human exonuclease 1 connects nucleotide excision repair (NER) processing with checkpoint activation in response to UV irradiation, Proc. Natl. Acad. Sci. U. S. A. 108 (2011) 13647–13652.
[54] T. Hishida, Y. Kubota, A.M. Carr, H. Iwasaki, RAD6-RAD18-RAD5-pathway-dependent tolerance to chronic low-dose ultraviolet light, Nature 457 (2009) 612–615.